Thermochimica Acta 491 (2009) 63–70

Contents lists available at ScienceDirect

Thermochimica Acta

journal homepage: www.elsevier.com/locate/tca

Isothermal crystallization and melting behavior of polypropylene/layered double hydroxide nanocomposites

Sunil P. Lonkar, R.P. Singh*

Division of Polymer Science and Engineering, National Chemical Laboratory, Pune 411008, Maharashtra, India

ARTICLE INFO

Article history:
Received 14 November 2008
Received in revised form 6 March 2009
Accepted 9 March 2009
Available online 19 March 2009

Keywords:
Polypropylene nanocomposites
Layered double hydroxide
Isothermal crystallization
Melting behavior

ABSTRACT

The effect of layered double hydroxide (LDH) nanolayers on the crystallization behavior of polypropylene (PP) was studied based on the preparation of nanocomposites by a melt intercalation method. The isothermal crystallization kinetics and subsequent melting behavior of PP/LDH hybrids were studied with differential scanning calorimetry (DSC), polarized optical microscopy (POM), and wide-angle X-ray diffraction (WAXD). Studies revealed that the LDH promoted heterogeneous nucleation, accelerating the crystallization of PP. The Avrami equation successfully describes the isothermal crystallization kinetics of PP/LDH hybrids and signifies heterogeneous nucleation in crystal growth of PP. The varying values of Avrami exponent (n) and half crystallization time ($t_{1/2}$) of PP and PP/LDH hybrids describes overall crystallization behavior. The crystallite size (D_{hkl}) and distribution of different crystallites in PP varied in presence of LDH. A significant increase in melting temperature is observed for PP/LDH hybrids. The POM showed that smaller and less perfect crystals were formed in nanocomposites because of molecular interaction between PP chains and LDH. The value of fold surface free energy (σ_e) of PP chains decreased with increasing LDH content. Finally, the overall results signify that LDH at nanometer level acted as nucleating agent and accelerate the overall crystallization process of PP.

1. Introduction

In recent years, polymer/layered crystal nanocomposites have been recognized as one of the most promising research field in material chemistry. The scientific and technological interest for tailoring and modifying the polymer properties has been driving a very vivid research on the nanostructured materials. In this regard, most emphasis has been given to polymer layered silicate nanocomposites, which after intercalation and exfoliation within the polymer structure, induces substantial increase in the material properties [1–3]. Recently, a new promising class of inorganic layered materials, layered double hydroxide (LDH) has been developed. The LDHs are the class of anionic or hydrotalcite like clays represented by the general formula $[M_{1-x}^{II}M_x^{III}(OH)_2]^{x+}.[(A^{n-})^{x/n}\cdot mH_2O]$ where M^{II} and M^{III} are divalent and trivalent metal cations, respectively, and A^- is the interlayer anion (Fig. 1) [4,5]. The typical metal hydroxide-like chemistry and conventional clay-like layered crystalline structure makes LDH potential flame retardant [6] and suitable for polymer nanocomposite preparation. In recent years, polymer/LDH nanocomposites have attracted a great interest because they exhibit improved physical and performance properties in comparison to the pristine polymers and conventional composites [7–11].

Polypropylene (PP) is one of the most widely used polyolefins and has stimulated intensive research in order to produce polypropylene nanocomposites with enhanced properties. Hence, it is important to investigate method of preparation, structure and properties of PP reinforced with LDH from commercial point of view. It is well understood that physical and mechanical properties of crystalline polymer like polypropylene depend on the morphology, crystalline structure and degree of crystallization. Therefore, the study of the kinetics of crystallization is necessary for optimizing industrial process, conditions and establishing the structure–property correlations in the case of PP/LDH nanocomposites. It was also recognized that some inorganic fillers, as reinforcing agents in composites, can induce nucleation for crystallization and overall crystallization process [12–14]. The isothermal and non-isothermal crystallization kinetics of PP and its composites with different fillers have been extensively reported in the literature [12–18]. It has been found that the degree of crystallinity, crystal size, and shape morphology and crystallization kinetics of the polypropylene matrix is strongly affected by the presence of nano-scale particulates. Recently, Chen et al. [13] calorimetrically studied the isothermal crystallization behavior of PP/polyhedral oligomeric silsesquioxane (POSS) nanocomposites and found that POSS nanoparticles could accelerate the overall crystallization of

* Corresponding author. Tel.: +91 20 25902091; fax: +91 20 25902615.
E-mail address: rp.singh@ncl.res.in (R.P. Singh).

0040-6031/$ – see front matter © 2009 Elsevier B.V. All rights reserved.
doi:10.1016/j.tca.2009.03.002

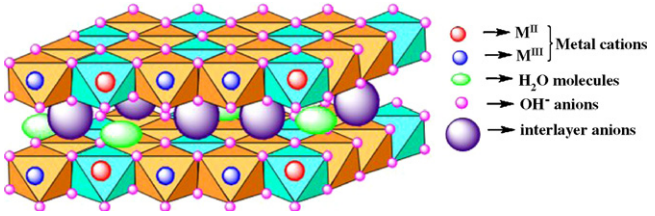

Fig. 1. Layered crystal structure of hydrotalcite-like compounds.

PP and suggested a three-dimensional growth with heterogeneous nucleation. Maiti et al. [18] investigated how crystallization controls of the fine structure and morphology of the PP/clay nanocomposites. They concluded that the clay platelets act as a nucleating agent and lower the size of the PP spherulites.

To our knowledge, only few articles report the use of such inorganic/organic (I/O) LDH/surfactant assemblies as filler for polymers and their effect on the iso or non-isothermal crystallization behavior and the subsequent effect on changes of the microstructural parameters [19–21]. However, there was no literature on studies of LDH induced isothermal crystallization and melting behavior of polypropylene. The purpose of this article was to investigate the influence of LDH type nanometric anionic clays, organo-modified by surfactant molecules as filler on the isothermal crystallization behavior of PP in PP/LDH hybrid nanocomposites. Melting behaviors following the isothermal crystallization process were also discussed. The layered structure and the dispersed morphology of LDH in PP matrix were confirmed by X-ray scattering (WAXD) and transmission electron microscopy (TEM), respectively. The data obtained from differential scanning calorimetry were employed for measuring crystallization kinetic parameters and subsequent melting. The crystallization kinetic parameters and thermal characteristics based on isothermal crystallization of the PP and PP/LDH composites were achieved by confronting Avrami equation. The spherulitic growth rate was used to obtain data on the specific surface free energies for the PP and all nanocomposites. The microcrystalline dimensions (D_{hkl}) of crystal growth and spherulitic morphology were investigated by WAXD and optical polarising microscopy (POM), respectively.

2. Experimental

2.1. Materials

The isotactic polypropylene used in this study is Exxon Mobile PP with 2.5–3.5 MFI. The maleic anhydride-grafted PP polymer (PP-g-MA) used as compatibilizer was a low molecular weight Polybond 3200 (MA content 1%, density 0.91 g/cm^3 and Mw 90,000) obtained from Chemtura corporation. Dodecyl sulfate modified LDH, i.e. Mg_2Al-DS LDH was prepared obtained through courtesy of Dr. Fabrice Leroux, University of Blaise Pascal, France.

2.2. Nanocomposite preparation

Nanocomposites containing 1%, 3% and 5% LDH nanoparticles were prepared by melt mixing in two steps using a co-rotating tightly intermeshed twin-screw extruder (DSM microcompounder). All materials were dried at 80 °C under vacuum prior to mixing.

2.2.1. Step 1: preparation of compatibilized PP

Isotactic polypropylene was mixed with MA-g-PP in a weight proportion of 95:5. The operation temperature was maintained at 180 °C for 5 min at 200 rpm rotor speed to prepare a master batch of compatibilizer in PP. All experiments were performed under inert atmosphere.

2.2.2. Step 2: preparation of composites

The designated amount of Mg_2Al-DS LDH was added to the molten compatabilized PP and mixed at 180 °C for 5 min keeping other parameters as above. The samples were abbreviated as PPL1, PPL3 and PPL5 for 1%, 3% and 5% loading in PP, respectively.

The films of thickness between 80 and 100 μm were obtained using laboratory press at 180 °C under 4 tonnes of pressure for 2 min.

2.3. Microstructure characterization

The degree of LDH nanolayer dispersion was analysed by WAXD with Rigaku (Japan) D/max-RB wide-angle X-ray diffractometer (WAXD). The operation parameters were Cu Kα radiation at a rotating anode generator operated at voltage of 40 kV and at current of 100 mA. The scanning rate was 2°/min at an interval of 0.02°. Samples for TEM imaging were sectioned using a Leica Ultracut UCT microtome at 80–100 nm thickness with a diamond knife at −100 °C. The sections were collected from water on 300 mesh carbon-coated copper grids. TEM imaging was done using a JEOL 1200EX electron microscope operating at an accelerating voltage of 100 kV. Images were captured using a charged couple detector camera and viewed using Gatan Digital Micrograph software.

2.4. Crystallization behavior

The isothermal crystallization kinetic measurements were carried out with a TA instruments Q10 differential scanning calorimeter (DSC) calibrated with indium. The samples of PP and PP/LDH nanocomposite about 200 μm thick were obtained by hot compression molding, disk-like samples about 5 mg weight were taken for DSC measurements. Samples were heated to 200 °C at a rate of 10 °C/min under a nitrogen atmosphere and held for 5 min to destroy any residual nuclei. Then it was rapidly cooled to certain isothermal crystallization temperatures (T_c), and held to allow complete crystallization. After the isothermal crystallization was finished, the samples were heated to 200 °C at a rate of 10 °C/min to estimate melting profile of the samples.

To support the isothermal crystallization events and kinetic results analyzed by DSC thermograms, a very thin section of samples were observed under crossed polarizers with a polarizing LEICA-DMRX optical microscopy (POM). A thin sample sandwiched between two glass cover slips was placed inside the Linkam shearing device (CSS450) and the temperature was raised to 200 °C at the rate of 30 °C/min, kept at that temperature for 5 min, and then rapidly cooled to 128 °C for isothermal crystallization for 20 min. The morphological features (optical texture images) were captured in Olympus CCD camera.

3. Result and discussion

3.1. Nanocomposite microstructure

The crystallization behavior of nanocomposites is strongly influenced by the dispersion state of nanolayers in polymer matrix, which can be analyzed from X-ray diffractions [22]. The complete disappearance of WAXD peaks may reveal high degree of exfoliation or the presence of small diffracting volume as in the cases of low filler loading. It must be taken into account that disappearance of diffraction peaks are not sufficient argument to recognize exfoliated structures. Direct observation by TEM is then necessary to characterize an exfoliation state. Fig. 2(a–d) shows WAXD analysis

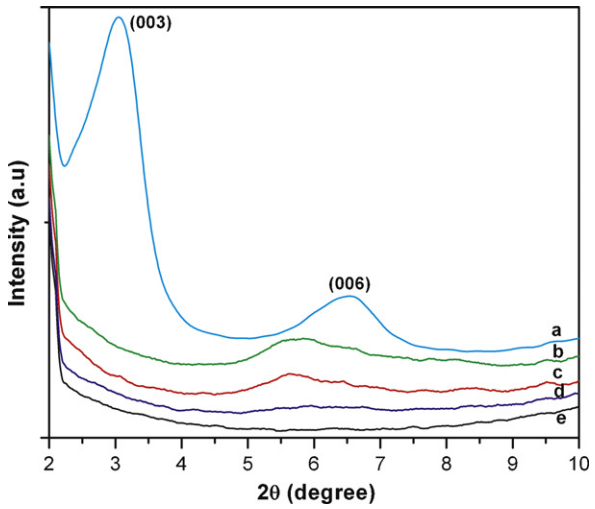

Fig. 2. The X-ray diffraction patterns of (a) Mg_2Al-DS LDH, (b) PPL5, (c) PPL3, (d) PPL1, and (e) PP in the range of $2\theta = 2–10^{\circ}$.

of PP and PP/LDH nanocomposites, a significant change in position of the basal peak was observed. The characteristic crystalline basal position peak of Mg_2Al-DS LDH at (003) (Fig. 2a) has been completely disappeared in case of PP/Mg_2Al-DS LDH nanocomposites (Fig. 2(b–d)). Moreover, the higher order basal position peak at (006) of PPL3 and PPL5 has been shifted towards lower angle and becomes broader. The overall WAXD results suggested that the stacking layers of the Mg_2Al-DS LDH in these samples were fully/partially separated and coexistence of both intercalated and exfoliated PP/LDH nanostructure was observed. To support these observations, the microstructure of the nanocomposites was investigated by TEM and micrographs are shown in Fig. 3(a and b), which confirm the fine dispersion of 5 wt% Mg_2Al-DS LDH in PPL5 sample. The micrograph shows that LDH nanolayers are well dispersed and intercalated throughout the PP matrix (Fig. 3a). Dark lines in the micrograph represent the LDH layers. From the TEM observations at high magnification (Fig. 3b), it is clear that the delamination took place resulting in the presence of single double hydroxide layers as well as tactoids with reduced thickness.

3.2. Isothermal crystallization

The crystallization kinetics of PP and PP/LDH nanocomposites were studied by differential scanning calorimetry (DSC). The DSC crystallization exotherms for PP and PP/LDH nanocomposites that had been isothermally crystallized at different crystallization temperatures (T_c) is shown in Fig. 4. It was observed that as the supercooling, i.e. the difference between the melting and crystallization temperature, decreases and the exothermal peak becomes broader which implies that the crystallization rate is reduced as the T_c increases. Thus, the induction time of the exotherm increases. The position of the crystallization peaks of PP/LDH nanocomposites appeared earlier than that of PP. It is evident that the crystallization rate of PP can be enhanced greatly by adding layered double hydroxides type nano-fillers. In the case of PP, the interval was between 118 and 126 °C and in the case of PP/LDH; this interval shifts to higher crystallization temperatures 122–130 °C. This shift revealed that the LDH nanolayers are acting as nucleating agent during the course of isothermal crystallization of PP. This phenomenon is in agreement with earlier reports describing effect of nano-fillers on crystallization behaviors of polypropylene [15,23]. However, the crystallinity value of PP in the nanocomposites is found to be almost independent of LDH content. Therefore, it can be concluded that the incorporation of the LDH increased the crystallization rate of PP chains without increasing the level of crystallinity.

In order to further analyze the isothermal crystallization process, the crystallization kinetics of PP and PP/LDH nanocomposites is compared. From dynamic crystallization experiments, data from the crystallization exotherms as a function of temperature; dH_c/dt can be obtained, for each crystallization temperature. The relative degree of crystallinity as a function of temperature, X_t, can be calculated according to the following equation:

$$X_t = \frac{\int_0^t (dH_c/dt)\ dt}{\int_0^{\infty} (dH_c/dt)\, dt} \tag{1}$$

where dH_c denotes the measured enthalpy of crystallization during and isothermal time interval dt. The limits t and ∞ denotes the elapsed time during the course of crystallization and at the end of the crystallization process, respectively. The development of relative degree of crystallinity X_t as a function of time, t, for PP and its nanocomposites at various crystallization temperatures is shown

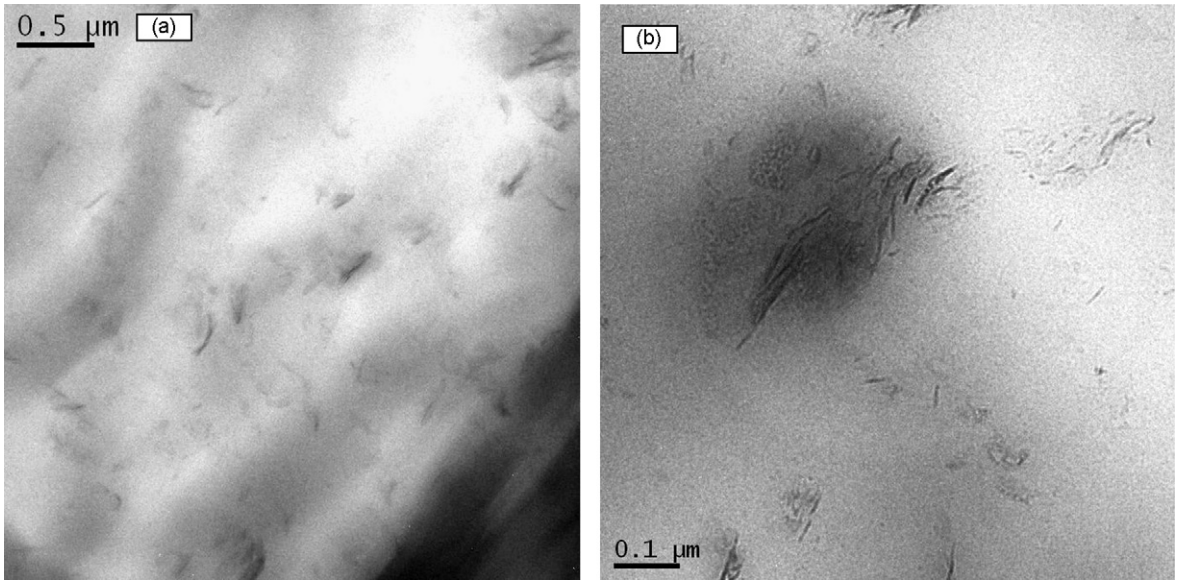

Fig. 3. TEM micrograph of PPL5 (a) 500 nm and (b) 100 nm magnifications.

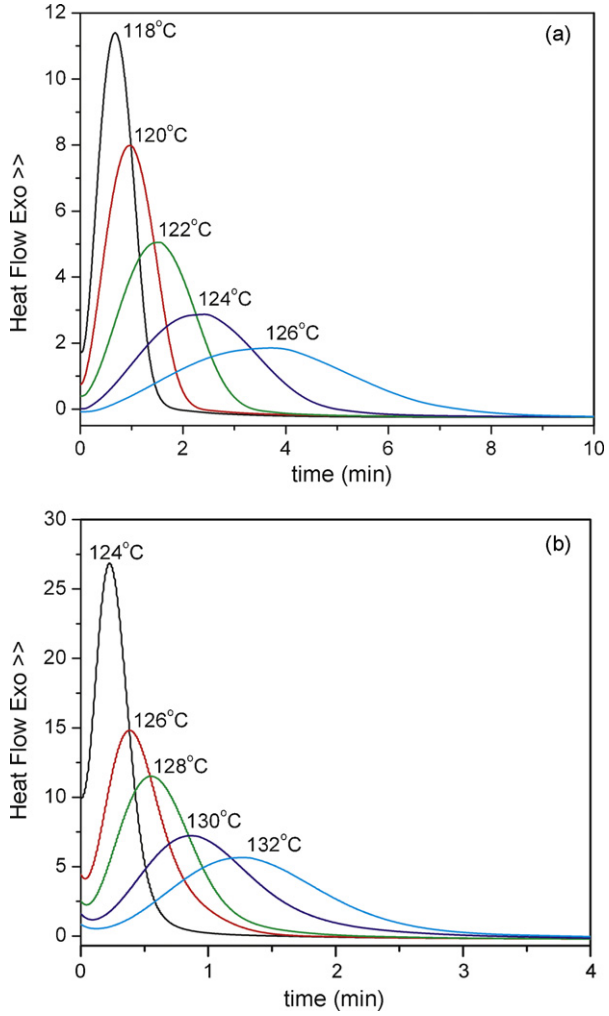

Fig. 4. DSC thermograms of isothermal crystallization at different crystallization temperature: (a) PP and (b) PPL5.

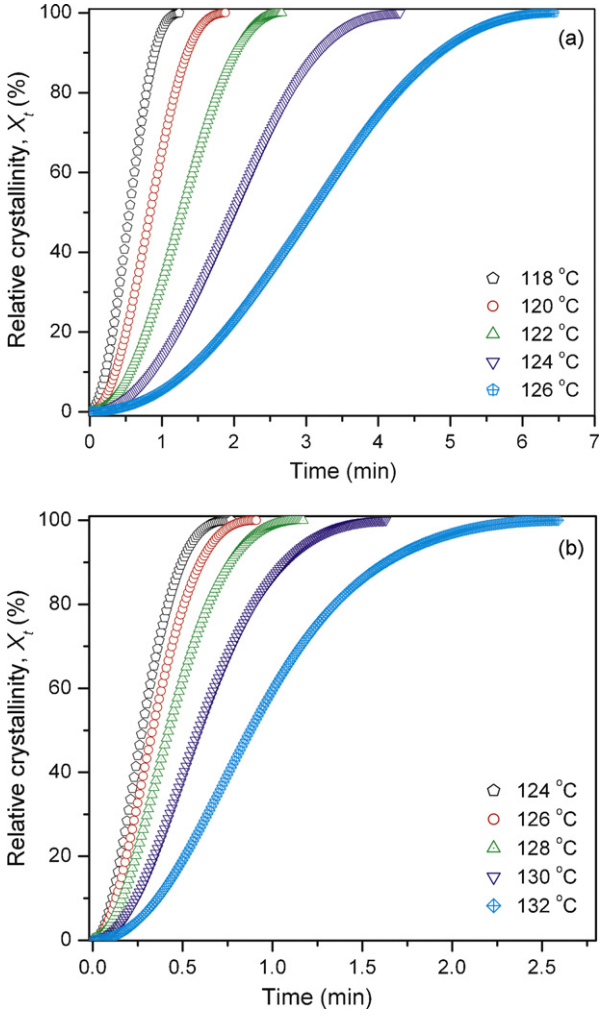

Fig. 5. The relative degree of crystallinity with time for the crystallization of (a) PP and (b) PPL5 at different crystallization temperatures.

in Fig. 5(a and b). The plots of X_t versus time for PP and PP/LDH (5%) nanocomposites are similar and all these curves have the same sigmoidal shape, implying that only a lag effect of temperature on crystallization is observed. The half crystallization time ($t_{1/2}$), which is direct measure of rate of crystallization can be defined as the half period (i.e. 50% crystallization), from the onset of crystallization and the end of crystallization. The $t_{1/2}$ values for PP and its nanocomposites can be obtained from Fig. 5, and the results are listed in Table 1. It is apparent that the value of $t_{1/2}$ decreases with increasing crystallization temperature. Moreover, at a given crystallization temperature, the $t_{1/2}$ value for PP/LDH nanocomposites is lower than that for PP and even decrease with increasing LDH content. The kinetic constant (k) of the PP/LDH hybrid is higher than that of PP at give crystallization temperature. These results signify that addition of Mg_2Al-DS LDH particles act as heterogeneous nucleating agents to facilitate the overall crystallization process.

Table 1
The Avrami parameters for isothermal crystallization of PP/LDH nanocomposites.

Sample	T_c (°C)	n	$k \times 10^{-2}$ (min^{-n})	T_m (°C)	$t_{1/2}$ (min)
PP	118	2.39	2.99	157.3	0.55
	120	2.40	1.17	157.5	0.84
	122	2.49	0.43	158.0	1.28
	124	2.52	0.134	158.7	2.0
	126	2.50	0.047	157.8	3.08
PPL5	124	2.01	28.18	163.2	0.33
	126	2.44	6.67	163.9	0.42
	128	2.28	3.98	164.1	0.59
	130	2.36	0.69	164.6	0.88
	132	2.51	0.28	165.1	1.09

In order to understand fully, the evolution of crystallinity during the isothermal crystallization, the Avrami model [24] was employed to analyze the isothermal crystallization kinetics of PP and its nanocomposites. As we know, the Avrami theory has been widely and successfully used for the interpretation of isothermal crystallization processes, according to which the equivalent time dependent crystallinity X_t can be expressed as,

$$X_t = 1 - \exp(-kt^n) \quad (2)$$

where X_t is relative degree of crystallinity at crystallization time t, n is the Avrami exponent and Z_t is the crystallization rate constant involving both nucleation and growth rate parameters. Eq. (2) can also be liberalized in its logarithmic form to give Eq. (3).

$$\log[-\ln(1 - X_t)] = \log k + n \log t \quad (3)$$

By fitting the experimental data to Eq. (3), the values of n and k can be obtained from the slope and intercept of the plots of $\log[-\ln(1 - X_t)]$ versus $\log t$ for each cooling rate shown in Fig. 6. The experimental data appear to fit very well with the Avrami equation at the primary crystallization stage, and plots of $\log[-\ln(1 - X_t)]$ versus $\log t$ at different T_c values and LDH content as it can be

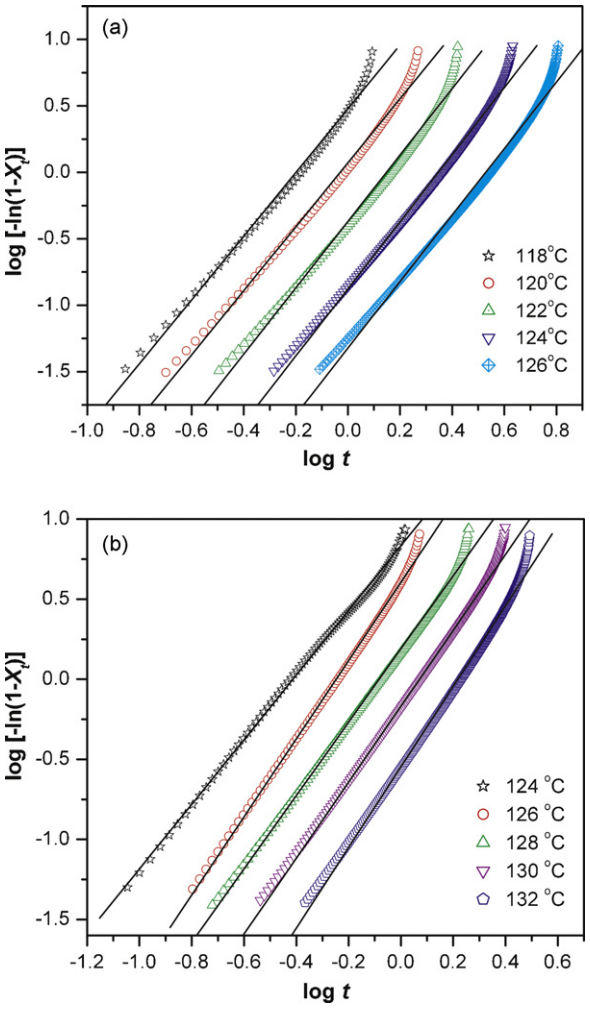

Fig. 6. Avrami plots of $\log[-\ln(1-X_t)]$ versus $\log t$ for isothermal crystallization process for (a) PP and (b) PPL5 nanocomposite.

seen straight lines are obtained showing good relationship at each cooling rate.

3.3. Crystal morphology

3.3.1. Crystalline structure of PP/LDH nanocomposites

The crystalline form and crystal size, markedly affects the mechanical properties of semicrystalline polymers like polypropylene. To investigate the influence of the LDH on the crystalline structure and crystallinity of PP, we performed WAXD experiments on both neat PP and the PP/LDH nanocomposites. Fig. 7 shows the WAXD intensity profiles of PP/LDH nanocomposites after isothermal crystallization at 128 °C. The X-ray diffractograms show nearly the α-crystalline form of PP after isothermal crystallization. The monoclinic α reflections of PP can be found at 2θ angles of 14.19° (1 1 0), 16.98° (0 4 0), 18.68° (1 3 0), 21.25° (1 1 1) and 21.91° (1 3 1 and 0 4 1) crystalline planes [25,26]. These observations confirm that the addition of LDH does not affect the crystalline polymorph of PP. However, the crystallization rate of PP is accelerated by the addition of LDH, as shown in the development of the WAXD crystalline reflections as a function of the crystalline time. In Fig. 7, it is also observed that the intensity of (1 1 0) plane decrease with increasing LDH content accompanied by increase in the intensity of (0 4 0) plane in case of nanocomposites. The intensity of (0 4 0) peak of PP in nanocomposites found increased because the surfaces of well-dispersed exfoliated LDH layers modified with organic modifier seems to induce the crystal growth in (0 4 0) direction. It is known that the ratio between the (1 1 0) and (0 4 0) gives the information on crystal growth orientations in a and b axes of α-phase [27]. The peak intensity of (1 1 0)/(0 4 0) in PP/LDH nanocomposites is not due to the possible change in the crystal forms, from α to γ form with addition of nano-filler like LDH which is in agreement with reports of Kim et al. [17] in case of maleated PP/MMT nanocomposites.

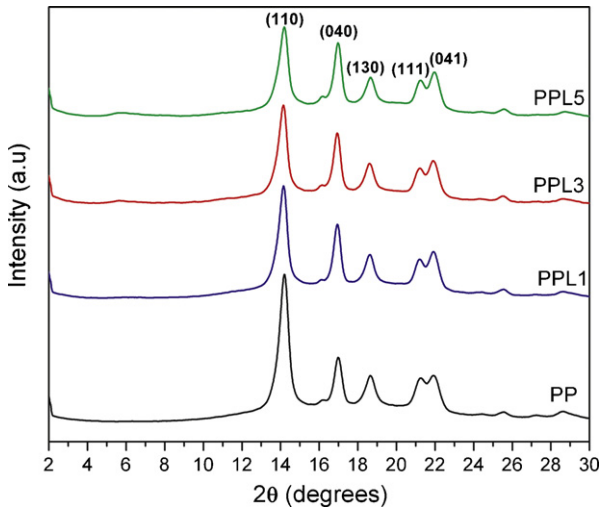

Fig. 7. X-ray diffractograms of isothermally crystallized nanocomposites: (a) PP, (b) PPL1, (c) PPL3 and (d) PPL5 at 128 °C.

The degree of perfection of the α-phase, i.e. crystalline size (D_{hkl}) can be calculated from the full width at half maximum (FWHM) of the (1 1 0) face using the Debye–Scherrer equation:

$$D_{h\,kl} = \frac{K\lambda}{\beta \cos\theta} \tag{4}$$

where D_{hkl} is the microcrystalline dimensions (nm), β is the half width of the diffraction peak in radian [$\beta = (\beta 1 - 0.2) \times \pi/180°$)], K is equal to 0.9, θ is the Bragg angle, and λ is the wave length of the X-rays ($\lambda = 0.154$ nm). The crystal sizes of the (1 1 0) planes of PP and its LDH hybrids obtained this equation are listed in Table 2. As can be seen, compared to PP, the crystal size of the composites is reduced, indicating that the packing order of the α-phase decreased in PP/LDH nanocomposites. This is in agreement with results obtained from POM study, which showed small size crystal formed with low degree of perfection.

3.3.2. Polarized light optical microscopy (POM)

In order to investigate the influence of LDH nano-particles on the morphology development and size of spherulites of PP, POM characterization was carried out. Fig. 8 shows the micrographs of PP and PPL5 after isothermally crystallizing at 128 °C for 15 min. One can observe well-defined spherulites with a 'Maltese-cross' structure for PP (Fig. 8a). Two kinds of optically different areas can be seen as separate phases. The dark and bright areas might be amorphous and crystal regions, respectively. Comparably, the morphology development of spherulites for PPL1, PPL3 and PPL5 shows

Table 2
The crystalline size $D_{1\,1\,0}$ of PP and PP/LDH hybrids.

	PP	PPL1	PPL3	PPL5
2θ (°)	14.2	14.15	14.15	14.19
$\beta 1$ (rad)	0.59	0.66	0.73	0.82
β (rad)	0.0068	0.0080	0.0092	0.010
$D_{1\,1\,0}$ (nm)	20.45	19.16	15.15	13.67

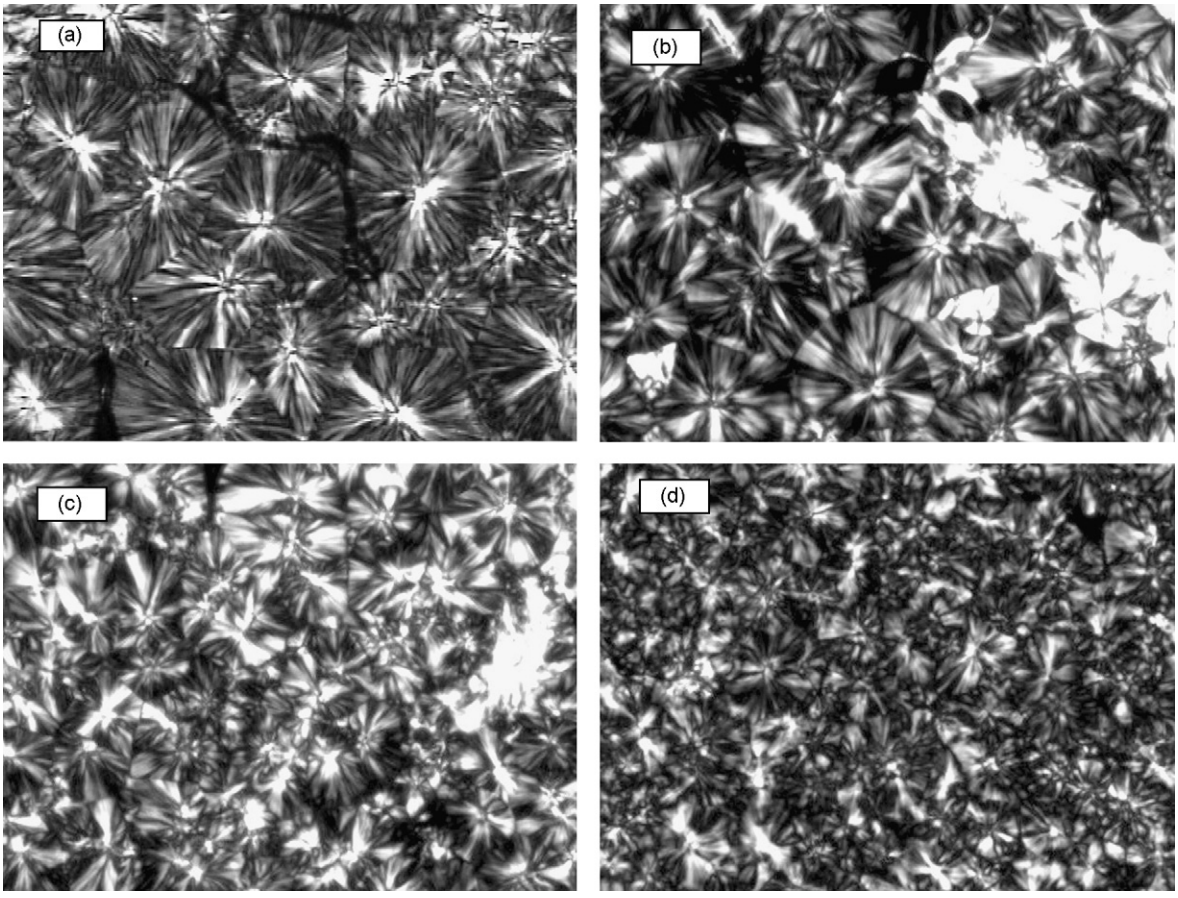

Fig. 8. Polarized microscopy pictures of isothermally crystallized nanocomposites: (a) PP, (b) PPL1, (c) PPL3 and (d) PPL5 at 128 °C.

the instantaneous nucleation process and there is little indication of any regular structure and have relatively small or less perfect Maltase crosses. Clearly, the dimensions of the spherulites decreases with LDH contents and only very tiny crystallites can be seen. This is due to the effect of the nano-dispersed LDH layers, which may act as seeds crystallization and may change the crystallization process during the formation of PP crystallites. Therefore, a gradual decrease in crystal growth and perfection has been observed with increasing LDH nanolayers in PP matrix.

3.4. Melting behavior and the crystallinity

The DSC heating thermograms of neat PP and the PP/LDH nanocomposite sample are presented in Fig. 9(a and b), respectively. It is observed that the PP/LDH nanocomposite DSC thermograms possess two melting peaks in contrast to the single melting peak of neat PP. However, the nature of the peak changes slightly with increasing crystallization temperature. While up to now, some discrepancies still existed in the origin and mechanism of the presence of multiple thermograms, it is generally believed that different thermal history leads to crystals with different perfection [28]. The cause of the first peaks in the scans thus is assumed to be due to the melting of the smallest lamellae produced by secondary crystallization and in the inter-lamellar layers between the larger crystallites. As such, this growth should not develop until after the primary stage is complete. Since the last peak is less dependent on the crystallization temperature and is much larger that the first one, it might be considered to be originated from the melting of the major crystals formed in the primary crystallization process [29].

As seen from Table 1, the crystallization temperature barely affected the melting profile of neat PP and its melting points were approximately at 157.6 °C at different crystalline temperature, whereas, the melting points of PP/LDH nanocomposites found higher than neat PP and was related to crystallization temperature. The melting of PPL5 crystallized at 132 °C was higher than that at 124 °C. Generally, the perfection of the crystalline, or high-temperature melting peaks increased with crystallization temperature, which was confirmed by the fact that the higher temperature melting peaks shifted to higher temperatures with higher crystallization temperature. Relatively imperfect crystals would be formed at lower crystallizations, and would melt at a lower temperature. This result indicates that the isothermal crystallization temperature influences the melting behavior of PP/LDH hybrid nanocomposites. The significant increase in melting points of nanocomposites could be ascribed due to possible interaction between LDH nanolayers and PP molecular chains.

3.5. Crystallization activation energy

The crystallization thermodynamics and kinetics of the nanocomposites have been analyzed on the basis of the theory of Hoffman–Lauritzen [30,31]. Accordingly, the crystal growth (G), depends on temperature, T, as follows:

$$G = G_0 \exp\left[-\frac{U*}{R(T_c - T_0)}\right] \exp\left[-\frac{K_g}{T_c\ \Delta Tf}\right] \quad (5)$$

where G_0 is the pre-exponential factor, U^* is the activation energy of the segmental jump, the first exponential term contains the contribution of diffusion process to the growth rate, while second exponential term is contribution of the nucleation process; U^* and T_0 are the Vogel–Fulcher–Tamman–Hesse (VFTH) parameters describing the transport of polymer segments

across the liquid/crystal interphase, $\Delta T = T_m - T_c$ the under cooling, $f = 2T_c(T_m + T_c)$ the correction factor. The universal values used for the VFTH parameters are $U^* = 1500$ cal/mol (6300 J/mol) and $T_0 = (T_g - 30)$ K [31]. In this study the T_g value of PP used was 270 K [32] and the equilibrium melting temperature T_m was set equal to 212.1 °C. This value found by Marand and coworkers [33] using non-linear Hoffman–Weeks extrapolation. The kinetic parameter, K_g is the term connected with the energy required for the formation of the nuclei of critical size and can be expressed as

$$K_g = \frac{nb\sigma\sigma_e T_m}{\Delta h_f k_B} \quad (6)$$

where n is the variable that considers the crystallization regime and assumes the value $n = 4$ for regimes I and III and $n = 2$ for regime II [34]. In the present work, the crystallization is assumed to take place in regime III according to Marand and coworkers [33], b is the distance between two adjacent fold planes taken as 6.26×10^{-10} m assuming (1 1 0) growth front [33], σ and σ_e are lateral and fold surface free energies, k_B is the Boltzmann constant ($k_B = 1.38 \times 10^{-23}$ J/K), $\Delta h_f = 1.93 \times 10^8$ is the heat of fusion per unit volume of crystal [35]. The nucleation parameter, K_g, can be calculated from Eq. (5) using double logarithmic transformation:

$$\ln G + \left[\frac{U*}{R(T_c - T_\infty)}\right] = \ln G_0 \left[-\frac{K_g}{T_c \Delta Tf}\right] \quad (7)$$

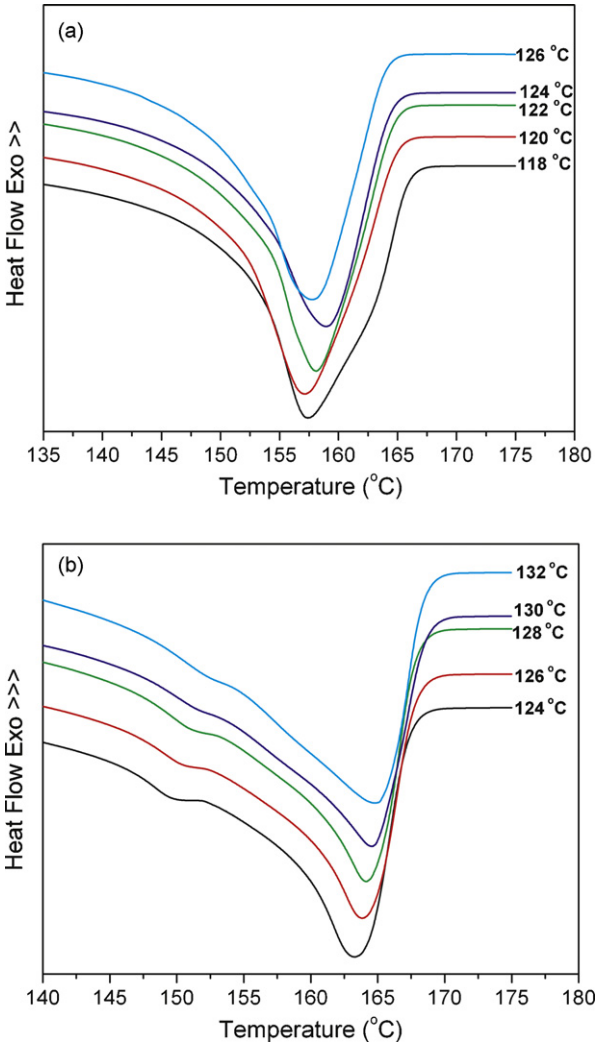

Fig. 9. Melting DSC curves of (a) PP and (b) PPL5 at different crystallization temperatures.

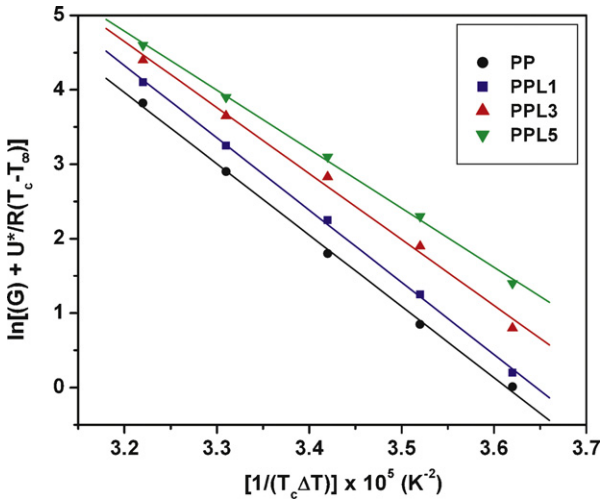

Fig. 10. Lauritzen–Hoffman type plots of $\ln G + U^*/(R(T_c - T_\infty))$ versus $1/(T_c - Tf)$ for PP and PP/LDH nanocomposites.

Table 3
Interfacial free energies (σ_e) and kinetic parameter (K_g) under isothermal crystallization process.

	K_g (10^5 K^2)	σ_e (erg/cm^2)
PP	10.21	125.3
PPL1	9.57	108.4
PPL3	8.85	94.2
PPL5	7.91	87.8

The plots of $\ln G + U^*/(R(T_c - T_\infty))$ versus $1/(T_c - Tf)$ are shown in Fig. 10 and shows that the experimental data can be reasonably fitted with straight lines. From the slope the value of K_g can be obtained. Eq. (6) were used to estimate the surface free energy (σ_e) and summarized in Table 3. There is clear tendency for σ_e to decrease with as the LDH content is increased. As it is well known, a foreign surface frequently reduces the nucleus size needed for crystal growth. The decrease of σ_e could indicate an increase in the entropy of folding and therefore the formation of less homogeneous and regular folding surface. As the composites have a higher melt viscosity than neat PP, the chain movements are restricted during crystallization and will form a less regular folding pattern in the crystals. Based on the results of PP/LDH nanocomposites we conclude that the addition of LDH at nanometric level reduces the creation of new surface, hence leading to faster crystallization rate.

4. Conclusion

The PP/LDH hybrid nanocomposites were prepared by melt intercalation method using PP-g-MA as a compatabilizer. The effect of LDH nanolayers on the crystal structure and isothermal crystallization behavior of PP in their nanocomposites were studied. It is observed that the addition of LDH remarkably affected the crystallization and melting behavior of PP/LDH hybrids. Kinetic parameters obtained from Avrami equation provided an adequate description of the isothermal crystallization behavior of PP/LDH nanocomposites. The values of Avrami exponent n varies from 2 to 2.5 for neat PP and PP/LDH nanocomposites, suggesting spherulitic crystal growth mechanism with heterogeneous nucleation. X-ray diffraction results indicated that the PP nanocomposites correspond to monoclinic α-form which implies the addition of LDH does not change the overall crystalline structure of PP. However, a slight decrease in microcrystalline dimensions is observed in case of PP/LDH hybrids. The melting behavior of PP is altered by addition of LDH, a significant increase and dual melting endotherms

are observed due to possible interaction between LDH nanolayers and PP molecular chains. The POM observations also reveal the decrease in size and perfection of PP spherulites due to nucleating effect of LDH. The value of fold surface free energy (σ_e) of PP chains decreased with increasing LDH content. Overall results conclude that the LDH at nanometer level can act as effective nucleating agent and accelerating crystallization rate of PP.

Acknowledgements

S. P. Lonkar is thankful to Council of Scientific and Industrial Research (CSIR), New Delhi, India, for granting senior research fellowship and also appreciates excellent characterization facilities at NCL, Pune.

References

[1] E.P. Giannelis, Appl. Organ. Chem. 12 (1998) 675–680.
[2] M. Alexandre, P. Dubois, Mater. Sci. Eng. 28 (2000) 1–63.
[3] S.S. Ray, M. Okamoto, Prog. Polym. Sci. 28 (2003) 1539–1641.
[4] V. Rives, Layered Double Hydroxides: Present and Future, Nova Publishers, New York, 2001.
[5] F.R. Costa, M. Saphiannikova, U. Wangenknechat, G. Henrich, Adv. Polym. Sci. 270 (2007) 101–168.
[6] M. Meyn, K. Beneke, G. Lagaly, Inorg. Chem. 29 (1990) 5201–5207.
[7] F.R. Costa, G. Abdel-Goad, U. Wangenknechat, G. Heinrich, Polymer 46 (2005) 4447–4453.
[8] M. Zammarano, S. Bellayer, J.W. Gilman, M. Franceschi, F.L. Beyer, R.H. Harris, Polymer 47 (2006) 652–662.
[9] M. Zammarano, M. Franceschi, S. Bellayer, J.W. Gilman, S. Meriani, Polymer 46 (2005) 9314–9328.
[10] F. Leroux, L. Meddar, B. Mailhot, S. Morlat-Therias, J.-L. Gardette, Polymer 46 (2005) 3571–3578.
[11] W.D. Lee, S.S. Im, H.M. Lim, K.J. Kim, Polymer 47 (2006) 1364–1371.
[12] W.B. Xu, M.L. Ge, P.S. He, J. Polym. Sci. Part B: Polym. Phys. 40 (2002) 408–414.
[13] J.-H. Chen, B.-X. Yao, W.-B. Su, Y.-B. Uang, Polymer 48 (2007) 1756–1769.
[14] Z. Zhou, L. Cui, Y. Zhang, Y. Zhang, N. Yin, J. Polym. Sci. Part B: Polym. Phys. 46 (2008) 1762–1772.
[15] M. Mucha, J. Marszalek, A. Fifrych, Polymer 41 (2000) 4137–4142.
[16] M. Naffakh, Z. Martin, M. Marco, M. Gomez, I. Jimenez, Themochim. Acta 472 (2008) 11–16.
[17] B. Kim, S.-H. Lee, D. Lee, B. Ha, J. Park, K. Char, Ind. Eng. Chem. Res. 43 (2004) 6082–6608.
[18] P. Maiti, P.H. Nam, M. Okamoto, N. Hasegawa, A. Usuki, Macromolecules 35 (2002) 2042–2049.
[19] W. Chen, B. Qu, Chem. Mater. 15 (2003) 3208–3213.
[20] P. Pan, B. Zhu, T. Dong, Y. Inoue, J. Polym. Sci. Part B: Polym. Phys. 46 (2008) 2222–2233.
[21] S.F. Hsu, T.M. Wu, C.S. Liao, J. Polym. Sci. Part B: Polym. Phys. 44 (2006) 3337–3347.
[22] A. Vermogen, K. Masenelli-Varlot, R. Seguela, J. Duchet-Rumeau, S. Boucard, P. Prele, Macromolecules 38 (2005) 9661–9669.
[23] M. Run, C. Yao, Y. Wang, J. Gao, J. Appl. Polym. Sci. 106 (2007) 1557–1567.
[24] M.J. Avrami, Chem. Phys. 8 (1940) 212–224.
[25] S. Bruckner, S.V. Meille, V. Petraccone, B. Pirozzi, Prog. Polym. Sci. 16 (1991) 361–404.
[26] R.A. Philips, M.D. Wolkowicz, in: E.P. Moore (Ed.), Polypropylene Handbook, Hanser, Munich, 1996, pp. 113–122.
[27] J. Wang, Q. Dou, Colloid Polym. Sci 286 (2008) 699–705.
[28] T. Liu, Z. Mo, S. Wang, H. Zhang, Eur. Polym. J. 33 (1997) 1405–1414.
[29] X.F. Lu, J.N. Hay, Polymer 42 (2001) 9423–9431.
[30] J.L. Lauritzen, J.D. Hoffman, J. Appl. Phys. 44 (2003) 4340–4344.
[31] J.D. Hoffman, R.L. Miller, Polymer 38 (1997) 3151–3212.
[32] Advance thermal analysis system (ATHAS databank), available from: http://web.utk.edu/athas/edu.
[33] J. Xu, S. Srinivar, H. Marand, P. Agarwal, Macromolecules 31 (1998) 8230–8242.
[34] E.J. Clark, J.D. Hoffman, Macromolecules 17 (1984) 878–885.
[35] H.S. Bu, S.Z.D. Cheng, B. Wundlich, Macromol. Rapid Commun. 9 (1988) 76–77.